Theory of Electrophoresis and Sedimentation for Some Kinetically Controlled Interactions†

John R. Cann* and Dale C. Oates

ABSTRACT: Theoretical electrophoretic and sedimentation patterns have been computed for several kinetically controlled macromolecular interactions: irreversible isomerization, dimerization, and dissociation into identical subunits, and irreversible and reversible dissociation of a complex. The latter calculations were designed to simulate the dissociation of an enzyme complex or a ribosome–enzyme complex. Both moving-boundary and zone patterns typically show two well-resolved peaks depending upon the rate of reaction, time of electrophoresis or sedimentation, and difference in velocity between reactants and products. A physical explanation for the resolution of reaction zones into two peaks is given, and an unambiguous method for distinguishing between reactions and inherent heterogeneity is described. Rate constants for irreversible reactions can be estimated with reasonable accuracy from analytical sedimentation patterns. In the case of isomerization or dissociation into subunits, but not dimerization, rate constants estimated from zone patterns are sufficiently accurate to be useful in pilot experiments.

Although there has been considerable interest within the past two decades in the electrophoresis, sedimentation, and chromatography of reversibly interacting macromolecules for which equilibration is rapid (Cann, 1970), rather less attention has been paid to kinetically controlled interactions, particularly irreversible ones. The two best understood kinetically controlled interactions are reversible isomerization (reaction I)

$$A \underset{k_2}{\overset{k_1}{\rightleftharpoons}} B \qquad (I)$$

(Keeler and Giddings, 1960; Giddings, 1960; Cann and Bailey, 1961; Scholten, 1961; Van Holde, 1962) and dimerization (reaction II)

$$2M \underset{k_2}{\overset{k_1}{\rightleftharpoons}} P \qquad (II)$$

(Belford and Belford, 1962; Oberhauser *et al.*, 1965) where k_1 and k_2 are the specific rates of reaction, and A and B have different mobilities. The unique feature of these systems is that their transport patterns may show three peaks for half-times of reaction comparable to the time of electrophoresis, sedimentation, or elution from a chromatographic column. Recently, the following questions have been asked of the authors: "Will the electrophoretic and sedimentation patterns of a macromolecule undergoing slow and irreversible isomerization, dimerization, or dissociation into subunits during the time course of the experiment show two peaks or a single skewed peak with a long trailing or leading edge?" and "Will the slow (either irreversible or reversible) dissociation of an enzyme complex or a ribosome–enzyme complex during the course of zone sedimentation give two peaks of enzymatic activity or a single skewed peak which trails?" In order to answer these questions we have made a theoretical investigation of the electrophoresis and sedimentation of such kinetically controlled processes. The results presented below predict two peaks for half-times of reaction ranging from about 0.3 to 2.5 times the duration of the experiment depending upon the difference in mobility between product and reactant. The greater the difference, the better is the resolution for longer half-times. There is no indication of single skewed peaks with long trailing or leading edges as long as the reaction does not go to completion during the course of the experiment.

Theory

Theoretical electrophoretic and sedimentation patterns of several kinetically controlled interacting systems have been computed by numerical solution of the appropriate conservation equations on a high-speed electronic computer using initial and boundary conditions corresponding to either moving-boundary or zonal modes of mass transport. The following macromolecular interactions have been examined: irreversible isomerization

$$A \xrightarrow{k} B \qquad (III)$$

dimerization

$$2M \xrightarrow{k} P \qquad (IV)$$

dissociation into identical subunits

$$P \xrightarrow{k} mM \qquad (V)$$

and both irreversible and reversible dissociation of a complex

$$C \underset{k_2}{\overset{k_1}{\rightleftharpoons}} A + B \qquad (VI)$$

† From the Department of Biophysics and Genetics, University of Colorado Medical Center, Denver, Colorado 80220. *Received October 16, 1972.* This work was supported in part by Research Grant No. 5R01 HL 13909-21 from the National Heart and Lung Institute, and Training Grant No. 5T01 GM 00781 from the National Institute of General Medical Sciences, National Institutes of Health, U. S. Public Health Service. This publication is No. 511 from the Department of Biophysics and Genetics, University of Colorado Medical Center.

where $k_2/k_1 \geqslant 0$ for the case $V_C = V_A > V_B$, where V_i is the velocity at which the ith species is driven by the applied field. The theory of moving-boundary electrophoresis, zone electrophoresis, and zone sedimentation through a linear density gradient is for rectilinear coordinates and constant velocities of the various species. The theory of analytical sedimentation in a sector-shaped cell is for cylindrically divergent coordinates and instantaneously varying velocities. The numerical procedures are outlined below.

Rectilinear Coordinates and Constant Velocities. To illustrate the procedures used in these calculations let us consider isomerization reaction III. It is assumed that during the course of electrophoresis of a macromolecule in solution it converts irreversibly from an initial state A to a new state B with a specific rate constant k, sec^{-1}. In the two states, A and B, the macromolecule migrates with electrophoretic mobilities μ_1 and μ_2 and diffuses with diffusion constants D_1 and D_2. The changes in concentrations of A and B, C_1 and C_2, expressed in either moles/liter or cgs units, with time of electrophoresis, t, and position in the electrophoresis column, x, are described by the system of forced diffusion equations

$$\frac{\partial C_1}{\partial t} = D_1\frac{\partial^2 C_1}{\partial x^2} - \mu_1 E\frac{\partial C_1}{\partial x} - kC_1 \quad (1a)$$

$$\frac{\partial C_2}{\partial t} = D_2\frac{\partial^2 C_2}{\partial x^2} - \mu_2 E\frac{\partial C_2}{\partial x} + kC_1 \quad (1b)$$

which make the assumption that D, μ, and the electric field strength, E, are the same throughout the electrophoresis column. These equations conserve mass by taking into account diffusion, transport in the electric field, and chemical reaction. Their solution gives the electrophoretic pattern of the reacting system. To this end we introduce the new time and position variables

$$t_0 = kt \quad (2a)$$

$$x_0 = (k/D)^{1/2}x - (k/D)^{1/2}\frac{(\mu_1 + \mu_2)E}{2}t \quad (2b)$$

$$D = D_1 = D_2 \quad (2c)$$

which transform eq 1a and 1b into

$$\frac{\partial C_1}{\partial t_0} = \frac{\partial^2 C_1}{\partial x_0^2} + \frac{1}{2(\alpha)^{1/2}}\frac{\partial C_1}{\partial x_0} - C_1 \quad (3a)$$

$$\frac{\partial C_2}{\partial t_0} = \frac{\partial^2 C_2}{\partial x_0^2} - \frac{1}{2(\alpha)^{1/2}}\frac{\partial C_2}{\partial x_0} + C_1 \quad (3b)$$

where

$$\alpha = \frac{Dk}{(\mu_2 - \mu_1)^2E^2} \quad (4)$$

We now introduce discrete time and position variables $t_0 = n\Delta t_0$, $n = 1, 2\ldots$, and $x_0 = j\Delta x_0$, $j = 1, 2\ldots J$, and replace the continuous variables $C_i(x_0, t_0)$ by the discrete variables $C_i(j\Delta x_0, n\Delta t_0) \equiv C_{i,j,n}$, $i = 1, 2$. Proceeding as in a previous investigation (Cann and Goad, 1965) the transformed eq 3a is approximated by the finite difference equation

$$C_{1,j,n+1} = C_{1,j,n} + \frac{\Delta t_0}{(x_0)^2}(C_{1,j+1,n} - 2C_{1,j,n} + C_{1,j-1,n}) + \frac{\Delta t_0}{2(\alpha)^{1/2}\Delta x_0}[\delta C_1]_{for} - \Delta t_0 C_{1,j,n} \quad (5)$$

in which

$$[\delta C_1]_{for} = C_{1,j+1,n} - C_{1,j,n} \text{ if } 1/2(\alpha)^{1/2} > 0$$

$$= C_{1,j,n} - C_{1,j-1,n} \text{ if } 1/2(\alpha)^{1/2} < 0$$

and similarly for eq 3b. Given the values of C_t at any time t, we can calculate their values at $t + \Delta t$ using eq 5. Thus, given initial conditions and boundary values, recursive solution of these equations in time allows one to follow the evolution of the electrophoretic pattern.

The initial conditions for moving-boundary electrophoresis are $C_{1,j,0} = 1$ and $C_{2,j,0} = 0, j = 1, 2\ldots J/2$, and $C_{1,j,0} = 0$ and $C_{2,j,0} = 0, j = J/2 + 1\ldots J$, and the boundary values are $C_{1,1,n} = C_{1,1,n-1} - \Delta t_0 C_{1,1,n-1}$, $C_{2,1,n} = C_{2,1,n-1} + \Delta t_0 C_{1,1,n-1}$, and $C_{1,J,n} = C_{2,J,n} = 0$. Ascending and descending electrophoresis for the case $\mu_2 > \mu_1$ is treated by choosing the signs of $1/2(\alpha)^{1/2}$ as positive and negative, respectively, and *vice versa* for $\mu_2 < \mu_1$.

For zone electrophoresis the initial conditions are $C_{1,j,0} = 1, j = J/2 - 5\ldots J/2 + 5$, $C_{1,j,0} = 0, j \neq J/2 - 5\ldots J/2 + 5$, and $C_{2,j,0} = 0, j = 1, 2\ldots J$, and the boundary values are $C_{1,1,n} = C_{2,1,n} = 0$ and $C_{1,J,n} = C_{2,J,n} = 0$.

As stated mathematically by the initial conditions given above, computations have been made for the case in which the macromolecule exists entirely in state A at the start of the electrophoresis experiment.

The foregoing mathematical formulation has been applied with only minor modifications to the other interactions which we have examined. The modifications which must be introduced can be summarized as follows.

(1) While in the case of isomerization the forced diffusion equations are the same whether concentrations are expressed in moles/liter or in cgs units, the dimensions of concentration must be specified for the other interactions. We have used molar concentrations which, in turn, requires that the dimensions of second-order rate constants be M^{-1} sec^{-1}.

(2) In the case of irreversible dimerization, reaction IV, the subscripts 1 and 2 designate the macromonomer M and its dimer P, respectively. The chemical kinetic terms in eq 1a and 1b are replaced by $-kC_1^2$ and $(1/2)kC_1^2$, respectively; eq 2c is replaced[1] by $D_2 = 2^{-1/3}D_1$, and D_1 replaces D in eq 2b and 4; eq 2a becomes $t_0 = kC_{10}t$, where C_{10} is the initial concentration of M; and kC_{10} replaces k in eq 2b and 4. The calculations are for the case in which all the macromolecule exists in its monomeric form at the beginning of the experiment.

(3) For irreversible dissociation of a macromolecule P into m identical subunits M, reaction V, the subscripts 1 and 2 designate P and M. The kinetic term in eq 1b is replaced by mkC_1; $D_2 = m^{1/3}D_1$; and D_1 replaces D in eq 2b and 4. Calculations are for pure P at the start of experiment.

(4) In the case of dissociation of a complex C into its macromolecular components A and B (reaction VI, $k_2/k_1 \geqslant 0$) the concentrations and transport parameters bear the subscripts 1, 2, and 3 to designate C, A, and B. There are three forced diffusion equations analogous to eq 1. The kinetic term

[1] We assume that diffusion coefficients vary inversely with the cube root of the molecular weight.

in the equation for C is $-k_1C_1 + k_2C_2C_3$; and in the equations for A and B, $k_1C_1 - k_2C_2C_3$. We have considered the case in which $D_1 = D_2 = D$, $D_3 = 10^{1/3}D$, and $\mu_1 = \mu_2 > \mu_3$. k_1 replaces k and μ_3 replaces μ_2 in eq 2a, 2b, and 4. The initial concentration of complex is designated as C_{10}, and the calculations are for pure C at the start of the experiment.

Computations were made on the University of Colorado's CDC 6400 electronic computer. Routinely we chose $\Delta x_0 = 0.3$ and $\Delta t_0 = 0.001$ which satisfy the stability criterion used previously (Cann and Goad, 1965). Decreasing the value of Δt_0 to 0.0005 had insignificant effect on the computed electrophoretic patterns, and decreasing Δx_0 to 0.1 caused only slight sharpening of the peaks in the patterns.

Computed moving-boundary patterns are displayed below as plots of concentration gradient [$\delta(C_1 + C_2)/\delta x_0$ in the case of isomerization, for example] against position, x_0. Zone patterns are plots of concentration [$4C_1 + C_2$ in the case of dissociation into four identical subunits] *vs.* x_0. In the case of dimerization, both concentration gradient and concentration have been normalized by the factor $1/C_{10}$.

The two vertical arrows in each pattern indicate where the peaks would have been located had electrophoresis been carried out on a mixture of noninteracting molecules having the same transport parameters as the reactant and product of the reacting system. In ascending moving-boundary patterns the arrow to the left is for the slower component, and migration may be viewed as occurring from left to right; in descending patterns, from right to left; and in zone patterns, from left to right.

Cylindrical Coordinates and Instantaneously Varying Velocities. The theory of analytical sedimentation will be illustrated for irreversible dimerization, reaction IV. The transport equation for sedimentation of this system in a sector-shaped cell is

$$\frac{\partial(C_1 + 2C_2)}{\partial t} = \frac{1}{r}\frac{\partial}{\partial r}\left[\left(D_1\frac{\partial C_1}{\partial r} - C_1 s_1\omega^2 r\right)r + 2\left(D_2\frac{\partial C_2}{\partial r} - C_2 s_2\omega^2 r\right)r\right] \quad (6)$$

in which s is the sedimentation coefficient; ω is the angular velocity, r is the radial distance, and concentrations have the dimensions moles/liter. This equation conserves mass by taking into account diffusion and transport in the centrifugal field. The rate equation

$$\frac{dC_1}{dt} = -kC_1^2 \quad (7)$$

in which k has the dimensions M^{-1} sec^{-1} expresses the effect of the chemical reaction on the concentration. Solution of simultaneous eq 6 and 7 gives the sedimentation pattern of the reacting system. To this end, we have adapted the numerical computation formulated by Goad (1970) for rapidly equilibrating ligand-mediated association–dissociation reactions. Essentially the adaptation consists of using Goad's finite difference approximation to eq 6 to compute changes in the concentrations of monomer and dimer due to radial dilution, driven transport, and diffusion during the time interval Δt. At each time step, after the concentrations have been advanced, new values of the concentrations as changed by irreversible chemical reaction (instead of reequilibration) are calculated using the integrated form of eq 7. The changes made in Goad's computer program to effect this adaptation are:[2] (1) in common and real statements replace K1 by the dummy variable KK; (2) following statement 36 in SUBROUTINE RADIUS insert the instruction C1(IS) = C1T; (3) following statement 38 in SUBROUTINE RADIUS insert C1(I) = C1T; (4) replace "CALL EQUIL" which appears below statement 36 and again below statement 38 in SUBROUTINE RADIUS by "CALL REACT"; and (5) change SUBROUTINE EQUIL to SUBROUTINE REACT retaining the common and real statements (with KK → K1) but replacing the instructions with

```
A = RK * DELT
C1(I) = C1(I)/(1.0 + C1(I)*A)
C2(I) = (CL(I) - Cl(I))/2.0
RETURN
END
```

In the first of these instructions RK is a Fortran name for k, but the numerical value of k was actually used here. A few words concerning input data are in order. Although our calulations are for the case in which all the macromolecule is in the form of monomer at the start of the experiment, a very small value (of the order of 10^{-14}) must be assigned to C21 in order to guard against dividing by zero in PROGRAM SEDMNT. For the same reason it is necessary to assign C31 = 1, s3 = 10^{-20}, and D3 = 10^{-20}, even though NUMSMA = 0.

With appropriate changes in SUBROUTINE REACT, the foregoing adaptation was also applied to irreversible isomerization by assigning MMER = 1.

Computed sedimentation patterns are displayed below as plots of concentration gradient against radial distance.

Results

Moving-Boundary Electrophoresis and Analytical Sedimentation. The course of development of the theoretical moving-boundary electrophoretic patterns for irreversible isomerization (reaction III, $\mu_2 > \mu_1$) is shown in Figure 1 for a case in which α (whose value depends among other things upon the difference in mobility of product and reactant) is 10^{-2}. The development of the patterns with increasing value of t_0 (*i.e.*, the product of k and time of electrophoresis) can be interpreted in two ways. The most natural interpretation is their evolution with time of electrophoresis for constant k and constant difference in the mobility of product and reactant. The conclusion to be drawn is that as time proceeds the pattern resolves into two peaks. The broad rapidly migrating peak, which corresponds largely to B, skews backwards in the direction from whence it was formed and increases in area with increasing time of electrophoresis. The sharp, slower peak corresponds to a mixture of A with some B; and its area decreases as electrophoresis and the chemical reaction proceed. In other words, the concentration of B changes with position throughout the pattern while the change in the concentration of A is largely restricted to the region of the slower peak and the minimum in the pattern. Moreover, the peaks migrate with velocities per unit field which differ from the mobilities of the individual isomers, and the gradient curve never reaches the base line between the peaks. It is thus evident that the two peaks constitute a single reaction boundary.

[2] In what follows, variables are denoted by their symbolic Fortran names as in Goad's program.

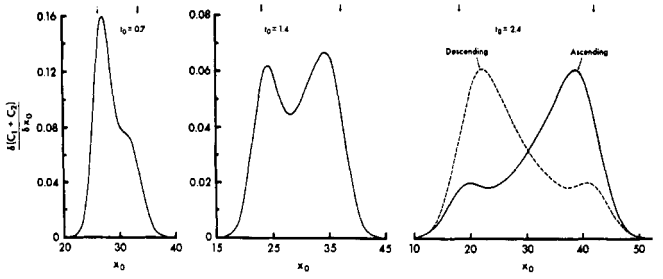

FIGURE 1: Theoretical moving-boundary electrophoretic patterns for irreversible isomerization, reaction III: (——) ascending patterns; (- - -), descending pattern; $\alpha = 10^{-2}$; $\mu_2 > \mu_1$. The pattern for $t_0 = 0.3$ shows only a slight indication of incipient resolution.

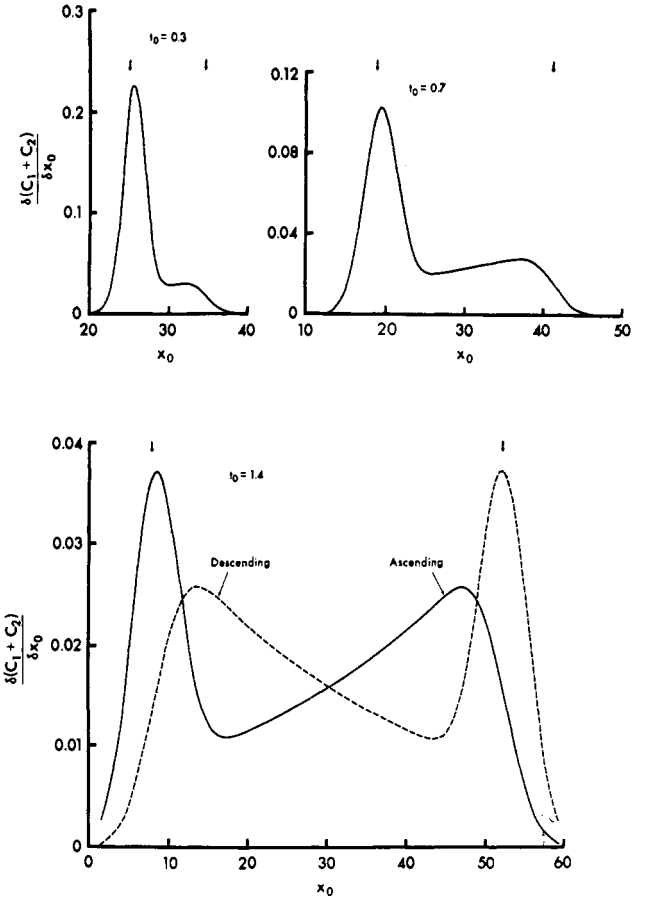

FIGURE 2: Theoretical moving-boundary electrophoretic patterns for irreversible isomerization; $\alpha = 10^{-3}$; $\mu_2 > \mu_1$.

The other interpretation of the development of the patterns with t_0 is their progressive change in shape with increasing rate of reaction at constant time of electrophoresis. (Since α remains constant as k increases, eq 4 tells us that the difference in the mobility between product and reactant must also increase.) When viewed in this way, it can be seen that for $\alpha = 10^{-2}$ resolution occurs only for half-times of reaction equal to or less than the time of electrophoresis, *i.e.*, for $t_0 \geq 0.7$. If, however, the value of α is decreased to 10^{-3}, which corresponds to slightly greater than a threefold increase in the difference in mobility between the isomers, resolution of the patterns is greatly enhanced (Figure 2). Indeed, resolution occurs even for a half-time of reaction 2.5 times greater than the time of electrophoresis ($t_0 = 0.3$, about 26% reaction during the course of electrophoresis). It is also apparent that increasing the difference in mobilities accentuates the skewing of the faster migrating peak, although the slower peak now migrates more nearly as the reactant. It can be concluded, therefore, that resolution into two peaks can occur for half-times of reaction ranging from about 0.3 to 2.5 times the duration of the experiment depending upon the difference in mobility between the isomers.

Finally, we note that ascending and descending patterns are enantiographic as might be expected for first-order kinetics of isomerization.

Quite similar results have been obtained for electrophoresis of an irreversibly dimerizing macromolecule (Figure 3A). In this case, however, the ascending and descending patterns are not mirror images, although the essential features are the same in both patterns. The nonenantiography is due to the fact that with second-order kinetics the fraction of macromolecule which dimerizes in a given time depends upon its concentration which, in turn, varies across the migrating front.

Estimates of the rate constant for isomerization or dimerization made from the areas of the peaks (defined by the concentration at the position of the minimum in the pattern) and the initial concentration of reactant are understandably low by 25–35% since the areas do not faithfully reflect the amounts of reactant and product. Nevertheless, this could be a valuable result of pilot experiments on a newly discovered system. On the other hand, it happens that much more accurate estimates can be made from sedimentation experiments.

Analytical sedimentation patterns computed for two different rates of irreversible isomerization are presented in Figure 4, and those for dimerization in Figure 5. One is impressed by the similarity of the sedimentation patterns and the corresponding electrophoretic patterns (Figures 1, 2, and 3A). It is interesting that the velocity of the slower peak (per unit centrifugal field) is the same to within about 2% as the sedimentation coefficient of isomer A or of the monomer, and that the velocity of the skewed faster peak, which is less than the sedimentation coefficient of isomer B or of the dimer, increases with time of sedimentation. Estimates of the rate constant made from the area of the slow peak and the initial concentration of reactant are low by only 5–10%. This relatively high degree of accuracy stems fortuitously from the coupling of the effect of radial dilution on the rate of chemical reaction and the differential transport of product and reactant. As a consequence, the area of the slow peak happens to approximate the instantaneous concentration of reactant had the reaction been carried out in a test tube.

Zone Electrophoresis and Sedimentation. Although the theory to be described below is formulated in terms of zone electrophoresis, the results are equally valid for zone sedimentation through a preformed linear density gradient in the preparative ultracentrifuge. This is so because macromolecules sediment with constant velocities under the conditions described by Martin and Ames (1961).

Theoretical zone patterns for irreversible isomerization are bimodal for appropriate rates of reaction and have the same shape as moving-boundary electrophoretic patterns. In fact, the moving-boundary patterns shown in Figures 1 and 2 can be translated into zone patterns simply by multiplying the ordinate scales by approximately 3 and changing their legends to read $C_1 + C_2$. Representative zone patterns for irreversible dimerization and for irreversible dissociation of a macro-

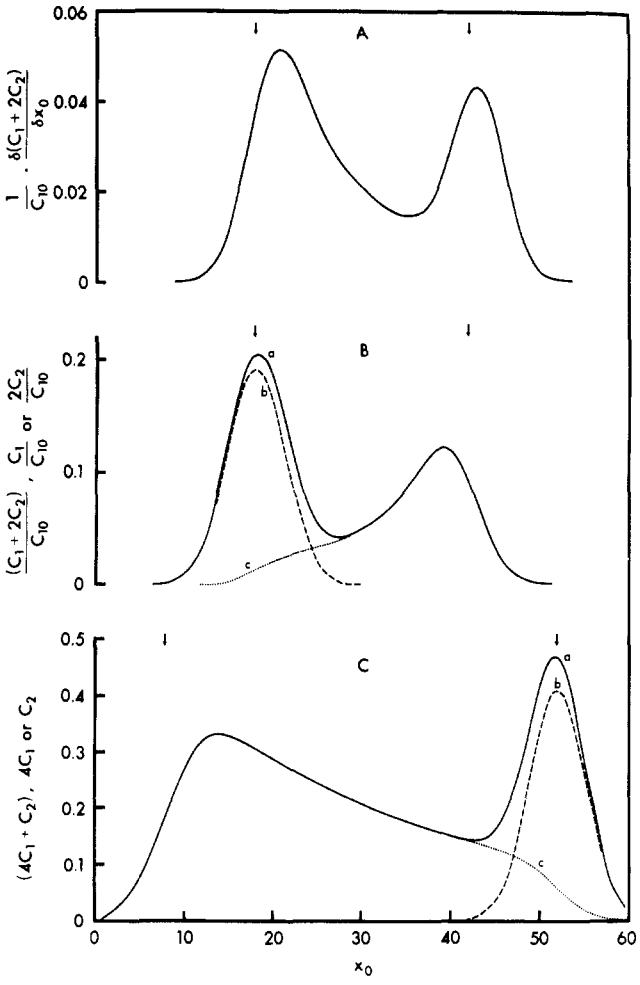

FIGURE 3: Theoretical transport patterns. (A) Descending moving-boundary electrophoretic pattern for irreversible dimerization, reaction IV, $\mu_2 > \mu_1$. (B) Zone electrophoretic or sedimentation pattern for irreversible dimerization: (a) total concentration, $(C_1 + 2C_2)/C_{10}$; (b) concentration of monomer, C_1/C_{10}; and (c) concentration of dimer, $2C_2/C_{10}$. (C) Zone electrophoretic or sedimentation pattern for irreversible dissociation into four identical subunits, reaction V ($m = 4$), $\mu_1 > \mu_2$: (a) total concentration, $4C_1 + C_2$; (b) concentration of tetramer, $4C_1$; (c) concentration of subunit, C_2; pattern was normalized by assigning unit initial concentration to P; essentially same pattern is shown for dissociation into halfmers, reaction V ($m = 2$).

molecule into four identical subunits are displayed in Figures 3B and 3C, respectively. The concentration profiles of reactant and product are also given in these figures. (It is not possible to translate moving-boundary patterns for dimerization into zone patterns because with second-order kinetics less reaction occurs in a spreading zone than in a plateau with a spreading front.) It is apparent that the two peaks in the various patterns are subject to essentially the same interpretation as given above for moving-boundary patterns and that they constitute a reaction zone. Also, the conditions for resolution are the same as described for moving-boundary electrophoresis, and there is no indication of single skewed peaks with long trailing or leading edges. Only if the reaction is sufficiently rapid so as to go to completion during the course of the experiment will the patterns show a single peak, which corresponds to product and is skewed in the direction from whence it was formed.

Rate constants for isomerization or dissociation into identical subunits estimated from the amounts of material in the

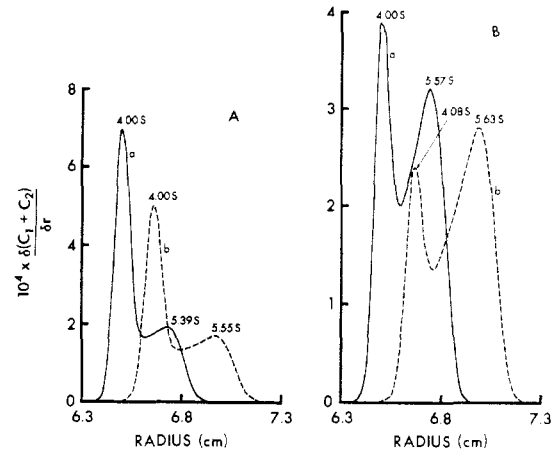

FIGURE 4: Theoretical analytical sedimentation patterns for irreversible isomerization, reaction III: (A) $k = 1.15 \times 10^{-4}$ sec^{-1}; (B) $k = 2.3 \times 10^{-4}$ sec^{-1}. Time of sedimentation: (a) 6098 sec; (b) 7623 sec. $C_{10} = 1.4 \times 10^{-4}$ M; $s_1 = 4$ S; $s_2 = 6$ S; $D_1 = 10^{-7}$ cm^2 sec^{-1}; $D_2 = 1.5 \times 10^{-7}$ cm^2 sec^{-1}; 60,000 rpm. Velocity per unit centrifugal field is shown above corresponding peak.

peak which is composed largely of product (as defined by the minimum in the pattern) are low by about 25%.[3] In the case of dimerization, such estimates are subject to unacceptable error.

Our calculations for dissociation of a complex into its macromolecular constituents (reaction VI, $k_2/k_1 \geq 0$) were designed to simulate the dissociation of either a large enzyme complex or ribosome–enzyme complex (C) to give a residual complex or ribosome (A) stripped of a particular enzyme molecule (B) which now exists in free solution. It is assumed that (1) the mobility of B is less than A which, in turn, is the same as C; (2) the molecular weight of B is only 10% that of C; and (3) the enzymatic activity per mole of C is the same as the activity per mole of B. The last two assumptions dictate that theoretical electrophoretic (or sedimentation) patterns be plots of $C_1 + 0.9C_2 + 0.1C_3$ (*i.e.*, total amount of material) or $C_1 + C_3$ (*i.e.*, enzymatic activity) against position. Representative patterns computed for two different values of the parameter α are presented in Figures 6 and 7 which also show the concentration profiles of the individual species. It is immediately apparent that the patterns are typically bimodal reaction zones depending upon the rates of reaction, time of electrophoresis, and difference between the mobility of complex and free enzyme. The faster migrating peak corresponds to a mixture of C, A, and B in the pattern of total material and to a mixture of C and B in the pattern of enzymatic activity, while in both cases the slower peak is comprised largely of B. The faster peak in the pattern of total material migrates with the same velocity as the complex, but the slower peak migrates faster than the free enzyme. In the pattern of enzymatic activity, the faster peak migrates slightly slower than the complex. The dependence of the shape of the zone

[3] Highly accurate values of first-order rate constants can be obtained by measuring the total amount of either reactant or product in the reaction zone. This is possible, for example, if one or the other has biological activity. But, measurements of this sort are best made in test-tube experiments after the nature of the reaction has been established by the combined application of zone centrifugation and other physical methods.

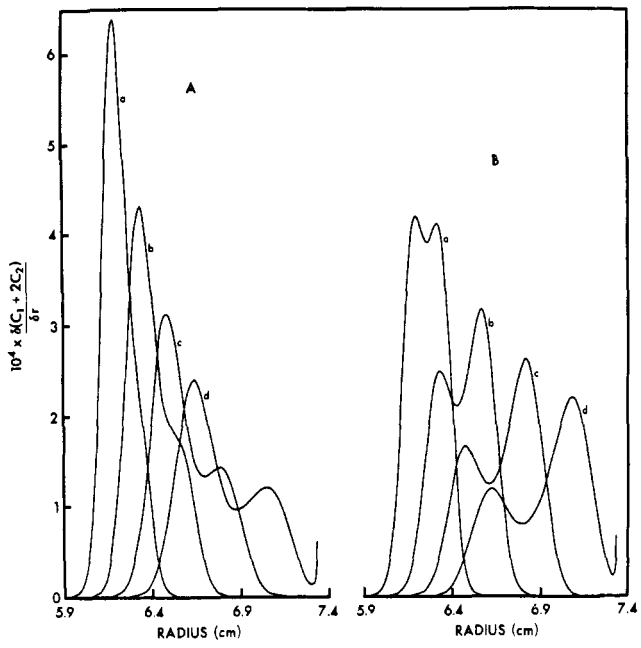

FIGURE 5: Theoretical analytical sedimentation patterns for irreversible dimerization, reaction IV: (A) $k = 1$ M^{-1} sec^{-1}; (B) $k = 3.33$ M^{-1} sec^{-1}. Time of sedimentation: (a) 3048 sec; (b) 4573; (c) 6097; (d) 7621. The velocities of the peaks (per unit centrifugal field) in A are: (a) 4.00 S; (b) 4.00 S; (c) 3.90 S and 5.75 S; (d) 3.92 S and 5.86 S. In B: (a) 4.00 S and 5.75 S; (b) 3.87 S and 5.94 S; (c) 3.90 S and 6.04 S; (d) 3.84 S and 6.10 S. $C_{10} = 1.4 \times 10^{-4}$ M; $s_1 = 4$ S; $s_2 = 6.35$ S; $D_1 = 6 \times 10^{-7}$ cm^2 sec^{-1}; $D_2 = 4.76 \times 10^{-7}$ cm^2 sec^{-1}; 60,000 rpm.

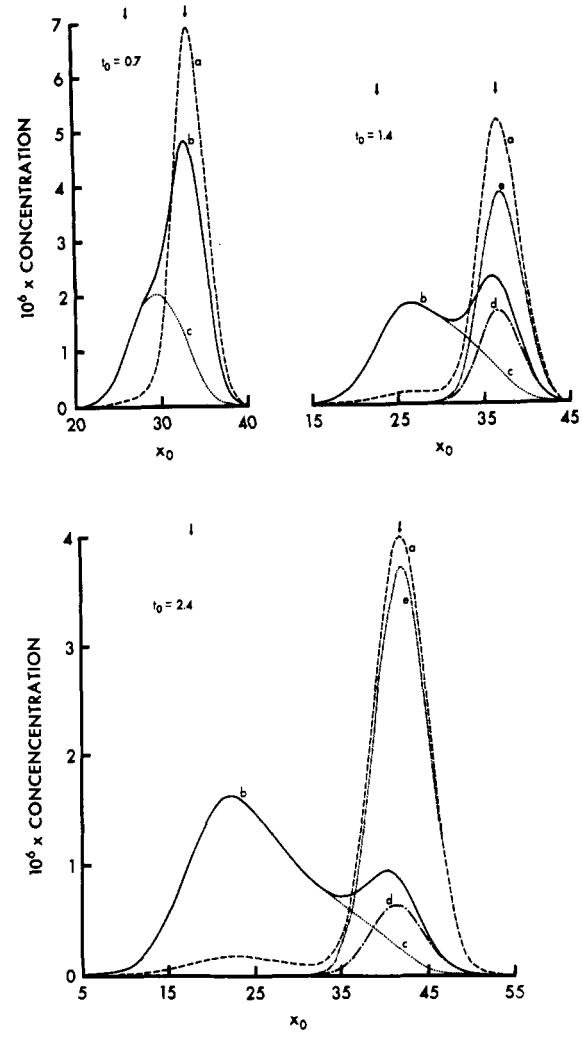

FIGURE 6: Theoretical zone electrophoretic or sedimentation patterns for dissociation of a complex, reaction VI, $\mu_1 = \mu_2 > \mu_3$: (a) $C_1 + 0.9C_2 + 0.1C_3$; (b) $C_1 + C_3$; (c) C_3; (d) C_1; (e) C_2. $\alpha = 10^{-2}$, $k_2/k_1 = 2 \times 10^5$ M^{-1}, $C_{10} = 10^{-5}$ M. The pattern for $t_0 = 0.3$ shows only slight indication of incipient resolution.

upon t_0 and upon α is much the same as in the case of irreversible isomerization and is subject to essentially the same interpretation. Thus, for example, resolution of the peaks improves markedly, particularly for slower rates of reaction, as the difference between the mobility of the complex and free enzyme increases. At the same time, the foreward skewing of the slower peak is accentuated. Single skewed peaks with trailing edges are never predicted for patterns of total material, and only if the reaction goes to completion during the course of electrophoresis will the pattern of activity show a single peak which is skewed forward. These results are for $k_2/k_1 = 2 \times 10^5$ M^{-1}. Those for $k_2/k_1 = 0$ (*i.e.*, irreversible dissociation) are practically the same, showing only minor differences in the heights of the several peaks due to slightly more dissociation of the complex during the course of electrophoresis.

Bimodal patterns of activity computed for values of k_2/k_1 ranging from 0 to 10^9 M^{-1} (other parameters held constant) are presented in Figure 8. These results show that the net amount of dissociation that occurs during the course of electrophoresis decreases with increasing specific rate of association. Thus, as k_2 increases at constant k_1, the faster migrating peak of activity grows progressively at the expense of the slower one. Another way of viewing these results is that the larger the association constant, the less reaction that occurs; but it must be borne in mind that these are kinetically controlled processes and that the concentrations of the several species in the fast peak of the pattern of total material approach equilibrium concentrations only at the highest values of k_2/k_1. Even for $k_2/k_1 = 10^7$ M^{-1}, the apparent association constant calculated from the concentrations in the fast peak is about 10% larger than the assigned values as compared to more than an order of magnitude larger for $k_2/k_1 = 2 \times 10^4$ M^{-1} and only 0.8% larger for $k_2/k_1 = 10^9$ M^{-1}. It is curious, therefore, that all the activity curves except for the one corresponding to $k_2/k_1 = 0$ pass through a common point reminiscent of an isosbestic point for absorption spectra. On the other hand, this is so only for $t_0 \leqslant 1.4$; for $t_0 = 2.4$, only those curves corresponding to $k_2/k_1 \geqslant 2 \times 10^6$ share a common point.[4]

Finally, we have explored the effect of initial concentration of complex upon the shape of the patterns. Decreasing C_{10} from 10^{-5} M to 2×10^{-6} M ($k_2/k_1 = 2 \times 10^5$ M^{-1}, $\alpha = 10^{-2}$) increases the amounts of complex that dissociate during transport, but to a lesser extent by about 50% than the increase cause by decreasing k_2/k_1 to zero at $C_{10} = 10^{-5}$ M. This is to be expected since some reassociation still occurs at the lower concentration.

[4] Careful scrutiny of the results of calculations for progressively smaller values of Δt_0 and Δx_0 clearly indicated that this partial loss of tie point is not due to propagation of truncation errors.

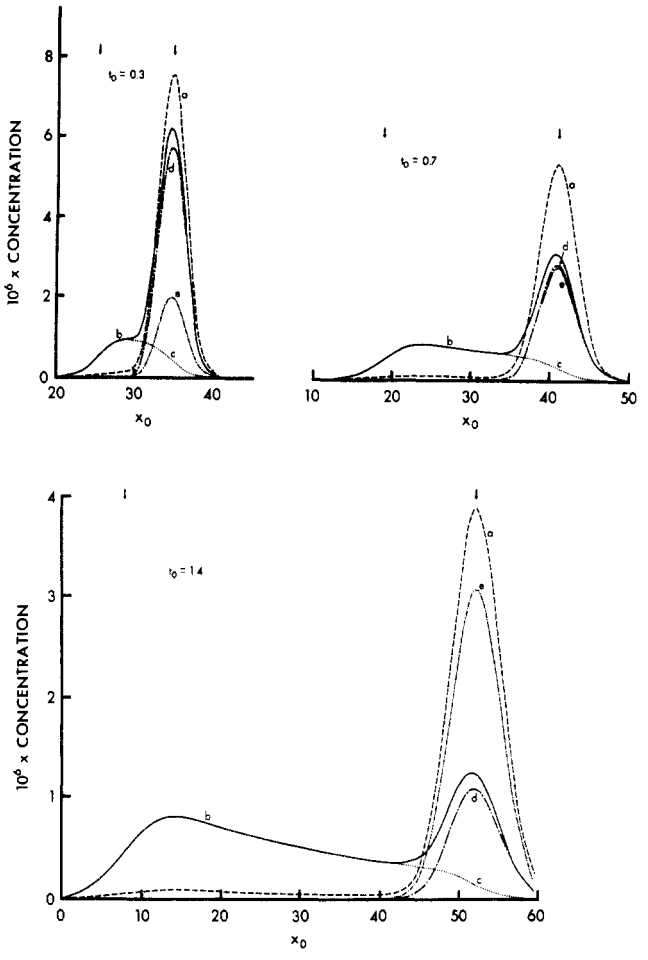

FIGURE 7: Theoretical zone electrophoretic or sedimentation patterns for dissociation of a complex: $\alpha = 10^{-3}$. Designation of the several curves is the same as in Figure 6.

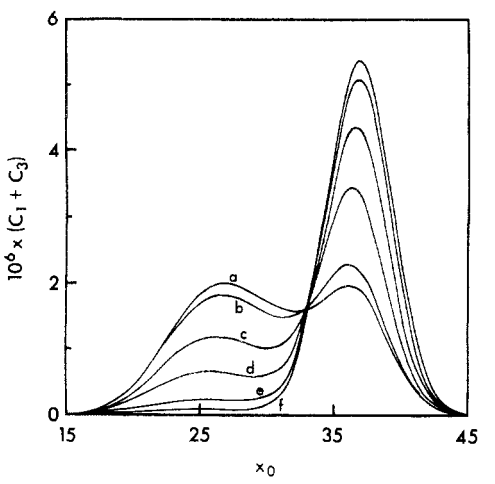

FIGURE 8: Theoretical zone electrophoretic or sedimentation patterns for dissociation of a complex. Plots of enzymatic activity, $C_1 + C_3$, against position for: (a) $k_2/k_1 = 0$; (b) 2×10^5 M^{-1}; (c) 2×10^6; (d) 10^7; (e) 10^8; (f) 10^9; $t_0 = 1.4$, $\alpha = 10^{-2}$, $C_{10} = 10^{-5}$ M.

Discussion

The theoretical electrophoretic and sedimentation patterns described above for several kinetically controlled interactions are typically bimodal reaction boundaries or zones. The physical explanation for resolution into two peaks is essentially the same for both moving-boundary and zonal transport. Consider, for example, zone sedimentation of an irreversibly reacting system in which the product has a smaller sedimentation constant than the reactant. As the zone of reactant departs from the meniscus and begins to sediment down the centrifuge tube, the reaction is occurring at its maximum rate determined by the initial concentration of reactant. Because of the difference in sedimentation velocity between product and reactant, the product lags behind the advancing peak of reactant and would form a long, trailing plateau if the reaction were to proceed at a constant rate. But, in fact, the rate of reaction decreases progressively with time as reactant is consumed. Since the amount of product formed per unit time decreases as differential sedimentation of product and reactant proceeds, the concentration profile of product must pass through a maximum and skew forward to blend into the peak of reactant. For the special case in which the rate of sedimentation of the product is negligibly small compared to the reactant, the maximum in its concentration profile will be located at the meniscus.

Inspection of the bimodal patterns presented in Figures 1–8 indicates that, in practice, at least some of them could easily be misinterpreted as indicative of a mixture of two stable, noninteracting macromolecules. Fortunately, however, fractionation provides an unambiguous method for distinguishing between reactions and inherent heterogeneity. In the fractionation test, the material in each peak is isolated and analyzed as in the original separation. For reactions of the sort considered here, the fraction comprised of product will migrate as a single peak while the one rich in reactant will exhibit two peaks like the unfractionated material. For heterogeneity, both fractions will run true. The fractionation test has recently been applied to the zone sedimentation of enzymatically active complexes between aminoacyl transferase I and proteinaceous cytoplasmic particles (Shelton *et al.*, 1970) and between aminoacyl-tRNA synthetases and ribosomes (Roberts, 1972).[5] The results revealed that the two peaks in the pattern of enzymatic activity do not correspond to isozymes with different molecular weights, but instead constitute a bimodal reaction zone arising from dissociation of the complex during the course of sedimentation.

Fractionation *per se* does not, however, provide information as to the rates of reaction, and one notes the striking similarities between the bimodal patterns displayed in Figure 6 for kinetically controlled (even irreversible) dissociation and those computed by Bethune and Kegeles (1961) for very rapid equilibration.[6] Even for pressure-induced reactions, such as the dissociation of ribosomes into subunits during sedimentation (Infante and Baierlein, 1971), it would be difficult to distinguish kinetic from equilibrium situations by zone sedimentation since the change in volume for activation is generally of the same magnitude as the charge accompanying the reaction (Benson, 1960). Thus, in both cases the shape of the zone pattern would be strongly dependent upon rotor speed, *i.e.*, the magnitude of the hydrostatic pressure generated in the centrifuge tube. On the other hand, it should be possible to distinguish the two by analytical sedimentation experiments

[5] Roberts, W. K. (1972), personal communication.

[6] These similarities are interpreted to mean that the difference in mobility between product and reactant is the dominant factor in determining the shape of the pattern.

in which the sample is overlayed with mineral oil (Josephs and Harrington, 1967); pressure-sensitive equilibria show reversible pressure effects upon rapid shifting of rotor speed (Morimoto and Kegeles, 1971).

Irreversible reactions which are not pressure induced can be identified by analyzing the fraction rich in reactant after it has been aged for varying lengths of time.

Finally, these results also apply with only quantitative reservations to molecular sieve chromatography on Sephadex or other gel permeation supports.

Acknowledgment

The authors express their appreciation to Dr. Walter B. Goad for his advice during the course of this investigation, and thank Mr. John L. McConnell for his technical assistance.

References

Belford, G. G., and Belford, R. L. (1962), *J. Phys. Chem. 37*, 1926.

Benson, S. W. (1960), The Foundations of Chemical Kinetics, New York, N. Y., McGraw-Hill, pp 510–517.

Bethune, J. L., and Kegeles, G. (1961), *J. Phys. Chem. 65*, 1755.

Cann, J. R. (1970), Interacting Macromolecules. The Theory and Practice of Their Electrophoresis, Ultracentrifugation, and Chromatography, New York, N. Y., Academic Press.

Cann, J. R., and Bailey, H. R. (1961), *Arch. Biochem. Biophys. 93*, 576.

Cann, J. R., and Goad, W. B. (1965), *J. Biol. Chem. 240*, 148.

Giddings, J. C. (1960), *J. Chromatogr. 3*, 443.

Goad, W. B. (1970), *in* Interacting Macromolecules. The Theory and Practice of Their Electrophoresis, Ultracentrifugation, and Chromatography, Cann, J. R., Chapter V, New York, N. Y., Academic Press.

Infante, A. A., and Baierlein, R. (1971), *Proc. Nat. Acad. Sci. 68*, 1780.

Josephs, R., and Harrington, W. F. (1967), *Proc. Nat. Acad. Sci. 58*, 1587 (1967).

Keeler, R. A., and Giddings, J. C. (1960), *J. Chromatogr. 3*, 205.

Martin, R. G., and Ames, B. N. (1961), *J. Biol. Chem. 236*, 1372.

Morimoto, K., and Kegeles, G. (1971), *Arch. Biochem. Biophys. 142*, 247.

Oberhauser, D. F., Bethune, J. L., and Kegeles, G. (1965), *Biochemistry 4*, 1878.

Scholten, P. C. (1961), *Arch. Biochem. Biophys. 93*, 568.

Shelton, E., Kuff, E. L., Maxwell, E. S., and Harrington, J. T. (1970), *J. Cell Biol. 45*, 1.

Van Holde, K. E. (1962), *J. Chem. Phys. 37*, 1922.

Structure of Immunoglobulin A. Amino Acid Sequence of Cysteine-Containing Peptides from the J Chain†

E. Mendez,* B. Frangione, and E. C. Franklin

ABSTRACT: A polymeric human IgA_1 myeloma protein (Oso) was partially reduced and alkylated with [^{14}C]iodoacetic acid. The J chain was isolated by several procedures. After partial reduction, at least eight cysteine-containing peptides were isolated and sequenced. Although the function and location of most of them remain unknown, one was shown to be the N-terminal peptide of the chain. The partial sequences of these carboxymethylcysteine peptides from the J chain indicated that they are different from those present in heavy and light chains. While this would suggest that the J chain has evolved independently, a possible relationship to the hinge region or other heavy-chain gene products whose structure is unknown deserves further study.

In 1970, Halpern and Koshland described the existence of a polypeptide chain in human and rabbit polymeric IgA[1] characterized by its rapid anodal mobility on alkaline urea gel electrophoresis. Shortly after, a similar chain was also observed in a Waldenstrom's macroglobulin (Mestecky *et al.*, 1971) and in proteins from several other species (Klaus *et al.*, 1971). In retrospect it would appear that this fast band had already been noted in secretory IgA in 1967 (Cebra and Small, 1967). Although its function remains unknown, its presence only in polymerized immunoglobulins suggests that it may serve to "join" the subunits and hence it was called the "J chain." Chemical studies of polymer IgA and IgM molecules and J chains have demonstrated that there is only one J chain per dimer (Morrison and Koshland, 1972) or pentamer (Mestecky *et al.*, 1971), that it is present only in polymeric IgA and IgM and not in monomeric IgA, and that it is rich in cysteine, containing approximately twice as much as light chains. Some question remains about the size of J chains since the molecular weight in sodium dodecyl sulfate polyacrylamide gel electrophoresis was 24,500, while

† From the Department of Medicine, Rheumatic Diseases Study Group, New York University School of Medicine, New York, New York. *Received September 25, 1972.* This work was supported by the Arthritis Foundation, Inc., USPHS Grants No. AM 01431, AM 05064, and AM 02594, and the Helen and Michael Shaffer Fund. E. M. is a postdoctoral fellow of the Damon Runyon Memorial Fund for Cancer Research.

[1] The nomenclature employed for the immunoglobulins follows that recommended by the World Health Organization, *Bull. W.H.O. 41*, 975 (1969).